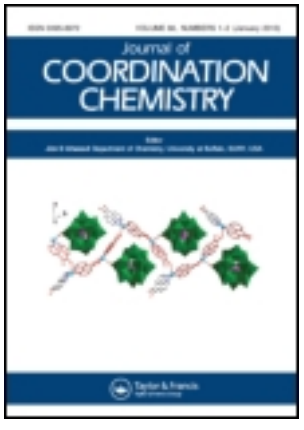

Journal of Coordination Chemistry
Publication details, including instructions for authors and subscription information:
http://www.tandfonline.com/loi/gcoo20

Triorganotin(IV) complexes with substituted benzeneseleninic acids: syntheses, characterization, crystal structures, and antitumor activity

Ru-Fen Zhang [a], Jing Ru [a], Zhen-Xing Li [a], Chun-Lin Ma [a b] & Jian-Ping Zhang [b]

[a] Department of Chemistry, Liaocheng University, Liaocheng 252059, P.R. China

[b] Department of Chemistry, Taishan University, Taian 271021, P.R. China

Published online: 21 Nov 2011.

To cite this article: Ru-Fen Zhang, Jing Ru, Zhen-Xing Li, Chun-Lin Ma & Jian-Ping Zhang (2011) Triorganotin(IV) complexes with substituted benzeneseleninic acids: syntheses, characterization, crystal structures, and antitumor activity, Journal of Coordination Chemistry, 64:23, 4122-4133, DOI: 10.1080/00958972.2011.637194

To link to this article: http://dx.doi.org/10.1080/00958972.2011.637194

Journal of Coordination Chemistry
Vol. 64, No. 23, 10 December 2011, 4122–4133

Triorganotin(IV) complexes with substituted benzeneseleninic acids: syntheses, characterization, crystal structures, and antitumor activity

RU-FEN ZHANG†, JING RU†, ZHEN-XING LI†, CHUN-LIN MA*†‡ and JIAN-PING ZHANG‡

†Department of Chemistry, Liaocheng University, Liaocheng 252059, P.R. China
‡Department of Chemistry, Taishan University, Taian 271021, P.R. China

(*Received 20 September 2011; in final form 17 October 2011*)

Nine new organotin(IV) selenites have been prepared by the reaction of 2-methylbenzeneseleninic acid, 2-methoxybenzeneseleninic acid, 4-isopropylbenzeneseleninic acid, and the corresponding triorganotin(IV) chloride with sodium ethoxide in methanol. The complexes have been characterized by elemental analysis, FT-IR, (^{1}H, ^{13}C, and ^{119}Sn) NMR spectroscopy, and thermogravimetric analysis. Except for **3**, **6**, and **9**, all of the complexes were also characterized by X-ray crystallography diffraction analyses. The structural analyses reveal that **1**, **2**, **4**, **5**, **7**, and **8** exhibit 1-D infinite chain structures which are generated by bidentate oxygen atoms and five-coordinated tin. Complex **5** forms a 2-D organotin framework linked by intermolecular C–H $\cdots$ O interactions. Additionally, **1** and **2** were tested for antitumor activity *in vitro*.

Keywords: Selenites; TGA; Triorganotin(IV); Antitumor activity

1. Introduction

Organotin complexes have attracted attention, partly owing to their wide industrial applications and biological activities [1, 2], and also due to the considerable structural diversity and various coordination numbers that they possess [3–5]. Owing to the vacant d orbital, tin can accept electrons from donors such as nitrogen, oxygen, or sulfur to form new complexes. Efforts have been done to synthesize a multitude of structural types, including monomers, dimers, tetramers, oligomeric ladders, hexameric drums, etc. [6, 7]. Although considerable advances have been made in the development of organotin complexes, relatively little work has been undertaken on the assembly of organotin clusters assisted by organoselenium ligands [8]. Selenium (Se) is an essential element for humans, primarily for its participation in redox homeostasis and as a promising cancer-chemopreventive agent [9–11]. In organic compounds, selenium is usually found in a divalent state with two covalently bonded substituents and two lone

*Corresponding author. Email: macl@lcu.edu.cn

ISSN 0095-8972 print/ISSN 1029-0389 online
http://dx.doi.org/10.1080/00958972.2011.637194

pairs of valence electrons. So when areneseleninic acids are administered as their metal complexes, biological activity is enhanced in comparison to the free ligand [12].

For the above considerations, we select 2-methylbenzeneseleninic acid, 2-methoxybenzeneseleninic acid and 4-isopropylbenzeneseleninic acid as ligands with the hope of triorganotin(IV) complexes with fascinating structures. We report herein the synthesis, spectroscopic analysis, thermogravimetric analysis (TGA), and X-crystallography of organotin(IV) derivatives of sub-areneseleninic acids.

2. Experimental

2.1. *Materials and measurements*

Trimethyltin chloride, tribenzyltin, and triphenyltin chloride are commercially available; sub-areneseleninic acids were prepared by a reported method [13, 14]. These were all used without purification. Melting points were obtained with a Kofler micro-melting point apparatus and are reported uncorrected. IR spectra were recorded with a Nicolet-5700 spectrophotometer using KBr discs and sodium chloride optics. ^{1}H (400 MHz), ^{13}C (100.6 MHz), and ^{119}Sn (149.2 MHz) NMR spectra were recorded on a Varian Mercury Plus-400NMR spectrometer. Chemical shifts are referenced to external tetramethylsilane (TMS) for ^{1}H and ^{13}C NMR and to neat tetramethyltin (Me_4Sn) for ^{119}Sn NMR. Elemental analyses were performed on a PE-2400-II elemental analyzer.

2.2. *X-ray crystallographic studies*

Crystals were mounted in Lindemann capillaries under nitrogen. Diffraction data were collected on a Smart CCD area-detector with graphite monochromated Mo-Kα radiation ($\lambda = 0.71073$ Å). A semi-empirical absorption correction was applied to the data. The structure was solved by direct methods using SHELXS-97 and refined against F^2 by full-matrix least-squares using SHELXL-97. Hydrogen atoms were placed in calculated positions. Crystal data and experimental details of the structure determinations are listed in tables 1 and 2.

2.3. *Syntheses of 1–9*

2.3.1. $[Me_3Sn(CH_3C_6H_4SeO_2)]_n$ (1). The reaction was carried out under nitrogen. 2-Methylbenzeneseleninic acid (0.203 g, 1 mmol) was added to methanol solution (30 mL) with sodium ethoxide (0.068 g, 1 mmol) and the mixture was stirred for 20 min, then trimethyltin chloride (0.199 g, 1 mmol) was added to the mixture and the reaction continued for 12 h at 50°C. After filtration the solvent was evaporated in vacuum and the residue was crystallized from methanol; colorless crystals were obtained. Yield: 75%; m.p. 150–153°C. Anal. Calcd for $C_{10}H_{16}SnO_2Se$: C, 32.82; H, 4.41. Found (%): C, 33.13; H, 4.56. IR (KBr, cm^{-1}): ν(Sn–C), 553.99; ν(Sn–O), 445.37. ^{1}H NMR [CD_3Cl, ppm]: δ 7.28–7.87(m, 4H, –Ph), 1.31(s, 3H, Ph–CH_3), 0.49(s, 9H, Sn–CH_3). ^{13}C NMR [CD_3Cl, ppm]: δ 122.13, 127.38, 131.45, 139.51 (Ar–C), 13.21 (Sn–CH_3). ^{119}Sn NMR [CD_3Cl, ppm]: −139.27.

Table 1. Crystal, data collection and structure refinement parameters for **1**, **2**, and **4**.

Complex	**1**	**2**	**4**
Empirical formula	$C_{10}H_{16}O_2SnSe$	$C_{50}H_{44}O_4Se_2Sn_2$	$C_{10}H_{16}O_3SnSe$
Formula weight	365.88	1104.15	381.88
Crystal system	Monoclinic	Orthorhombic	Monoclinic
Space group	c2/c	p212121	p21/c
Unit cell dimensions (Å, °)			
a	12.2933(11)	10.6502(13)	10.3057(11)
b	10.3805(10)	18.794(2)	9.7558(9)
c	20.768(2)	22.921(3)	14.4413(12)
α	90	90	90
β	104.6970(10)	90	110.6830(10)
γ	90	90	90
Volume (Å^3), *Z*	2563.5(4), 8	4587.9(9), 4	1358.4(2), 4
Calculated density (Mg m^{-3})	1.896	1.599	1.867
Absorption coefficient (mm^{-1})	4.809	2.718	4.547
F(000)	1408	2176	736
Crystal size (mm^3)	$0.27 \times 0.18 \times 0.15$	$0.24 \times 0.21 \times 0.16$	$0.36 \times 0.19 \times 0.18$
Reflections collected	6566	23,422	6671
Unique reflections [R_{int}]	2272 [R(int) = 0.0410]	7928 [R(int) = 0.0652]	2384 [R(int) = 0.0314]
Data/restraints/parameters	2272/0/131	7928/0/523	2384/0/140
Goodness-of-fit on F^2	1.012	0.971	
Final R indices [$I > 2\sigma(I)$]	$R_1 = 0.0247$, $wR_2 = 0.0563$	$R_1 = 0.0431$, $wR_2 = 0.0833$	$R_1 = 0.0218$, $wR_2 = 0.0507$
R indices (all data)	$R_1 = 0.0354$, $wR_2 = 0.0612$	$R_1 = 0.0704$, $wR_2 = 0.0942$	$R_1 = 0.0319$, $wR_2 = 0.0542$

Table 2. Crystal, data collection and structure refinement parameters for **5**, **7**, and **8**.

Complex	**5**	**7**	**8**
Empirical formula	$C_{100}H_{88}O_{12}Se_4Sn_4$	$C_{12}H_{20}O_2SeSn$	$C_{27}H_{26}O_2SnSe$
Formula weight	2272.30	393.93	580.13
Crystal system	Monoclinic	Triclinic	Monoclinic
Space group	p21	$P\bar{1}$	p21/n
Unit cell dimensions (Å, °)			
a	11.3157(13)	10.1980(10)	12.5854(12)
b	38.185(3)	13.3191(12)	12.5680(11)
c	11.3671(11)	22.805(2)	15.8206(16)
α)	90	85.5920(10)	90
β	101.9040(10)	89.1730(10)	101.3820(10)
γ	90	89.130(2)	90
Volume (Å^3), *Z*	4806.0(8), 2	3087.8(5), 8	2453.2(4), 4
Calculated density (Mg m^{-3})	1.570	1.695	1.571
Absorption coefficient (mm^{-1})	2.600	3.999	2.546
F(000)	2240	1536	1152
Crystal size (mm^3)	$0.19 \times 0.16 \times 0.13$	$0.13 \times 0.12 \times 0.06$	$0.36 \times 0.28 \times 0.15$
Reflections collected	25,242	15,777	12,070
Unique reflections [R_{int}]	16602 [R(int) = 0.0416]	10731 [R(int) = 0.1145]	4315 [R(int) = 0.0372]
Data/restraints/parameters	16,602/1/1085	10,731/283/595	4315/0/282
Goodness-of-fit on F^2	1.059	1.224	1.059
Final R indices [$I > 2\sigma(I)$]	$R_1 = 0.0593$, $wR_2 = 0.1458$	$R_1 = 0.1688$, $wR_2 = 0.4426$	$R_1 = 0.0283$, $wR_2 = 0.0582$
R indices (all data)	$R_1 = 0.0717$, $wR_2 = 0.1507$	$R_1 = 0.2891$, $wR_2 = 0.4890$	$R_1 = 0.0489$, $wR_2 = 0.0690$

2.3.2. $[Ph_3Sn(CH_3C_6H_4SeO_2)]_n$ (2). The procedure is similar to that of **1**, 2-methylbenzeneseleninic acid (0.203 g, 1 mmol), sodium ethoxide (0.068 g, 1 mmol), and triphenyltin chloride (0.385 g, 1 mmol) were reacted for 12 h at 50°C. Recrystallized from ether, transparent colorless crystals were formed. Yield: 70%; m.p. 232–235°C. Anal. Calcd for $C_{50}H_{44}Sn_2O_4Se_2$: C, 54.39; H, 4.02. Found (%): C, 54.63; H, 3.81. IR (KBr, cm^{-1}): ν(Sn–C), 580.36; ν(Sn–O), 454.29. ^{1}H NMR [CD_3Cl, ppm]: δ 7.09–7.87 (m, 38H, –Ph), 1.29 (s, 6H, Ph-CH_3). ^{13}C NMR [CD_3Cl, ppm]: δ 121.22–143.38 (Ar–C). ^{119}Sn NMR [CD_3Cl, ppm]: −143.72.

2.3.3. $[(PhCH_2)_3Sn(CH_3C_6H_4SeO_2)]_n$ (3). The procedure is similar to that of **1**, 2-methylbenzeneseleninic acid (0.203 g, 1 mmol), sodium ethoxide (0.068 g, 1 mmol), and $(PhCH_2)_3SnCl$ (0.427 g, 1 mmol) were reacted for 12 h at 50°C. Recrystallized from ether, white powder was formed. Yield: 70%; m.p. 223–226°C. Anal. Calcd for $C_{28}H_{28}SnO_2Se$: C, 56.60; H, 4.75. Found (%): C, 56.35; H, 4.37. IR (KBr, cm^{-1}): ν(Sn–C), 562.37; ν(Sn–O), 451.76. ^{1}H NMR [CD_3Cl, ppm]: δ 7.11–7.90 (m, 38H, –Ph), 1.32 (s, 6H, Ph–CH_3). ^{13}C NMR [CD_3Cl, ppm]: δ 121.29–144.16 (Ar–C), 37.6 (CH_2–Ph). ^{119}Sn NMR [CD_3Cl, ppm]: −138.13.

2.3.4. $[Me_3Sn(CH_3OC_6H_4SeO_2)]_n$ (4). The procedure is similar to that of **1**, 2-methoxybenzeneseleninic acid (0.229 g, 1 mmol), sodium ethoxide (0.068 g, 1 mmol), and trimethyltin chloride (0.199 g, 1 mmol) were reacted for 12 h at 50°C. Recrystallized from ether-petroleum ether formed transparent colorless crystals. Yield: 71%; m.p. 166–168°C. Anal. Calcd for $C_{10}H_{16}SnO_3Se$: C, 31.45; H, 4.22. Found (%): C, 29.12; H, 4.51. IR (KBr, cm^{-1}): ν(Sn–C), 565.76; ν(Sn–O), 454.29. ^{1}H NMR [CD_3Cl, ppm]: δ 7.15–7.62 (m, 4H, –Ph), 3.33 (s, 3H, Ph–O–CH_3), 0.44 (m, 9H, Sn–CH_3). ^{13}C NMR [CD_3Cl, ppm]: δ 115.38, 124.83, 129.81, 138.50, 162.27 (Ar–C), 51.74 (O–CH_3), 15.98 (Sn–CH_3). ^{119}Sn NMR [CD_3Cl, ppm]: −146.58.

2.3.5. $[Ph_3Sn(CH_3OC_6H_4SeO_2)]_n$ (5). The procedure is similar to that of **1**, 2-methoxybenzeneseleninic acid (0.229 g, 1 mmol), sodium ethoxide (0.068 g, 1 mmol), and triphenyltin chloride (0.385 g, 1 mmol) were reacted for 12 h at 50°C. Recrystallized from ether-dichloromethane, transparent colorless crystals were formed. Yield: 66%; m.p. 228–231°C. Anal. Calcd for $C_{25}H_{22}SnO_3Se$: C, 52.85; H, 3.90. Found (%): C, 52.59; H, 4.12. IR (KBr, cm^{-1}): ν(Sn–C), 568.23; ν(Sn–O), 442.19. ^{1}H NMR [CD_3Cl, ppm]: δ 6.82–7.36 (m, 19H, –Ph), 3.63 (s, 3H, Ph–O–CH_3). ^{13}C NMR [CD_3Cl, ppm]: δ 120.36–141.97 (Ar–C), 29.68 (Ph–O–CH_3). ^{119}Sn NMR [CD_3Cl, ppm]: −152.78.

2.3.6. $[(PhCH_2)_3Sn(CH_3OC_6H_4SeO_2)]_n$ (6). The procedure is similar to that of **1**, 2-methoxybenzeneseleninic acid (0.229 g, 1 mmol), sodium ethoxide (0.068 g, 1 mmol), and $(PhCH_2)_3SnCl$ (0.427 g, 1 mmol) were reacted for 12 h at 50°C. Recrystallized from ether-dichloromethane, white powder was formed. Yield: 66%; m.p. 226–228°C. Anal. Calcd for $C_{28}H_{28}SnO_3Se$: C, 55.11; H, 4.63. Found (%): C, 54.88; H, 4.89. IR (KBr, cm^{-1}): ν(Sn–C), 535.21; ν(Sn–O), 475.32. ^{1}H NMR [CD_3Cl, ppm]: δ 6.80–7.29 (m, 19H, –Ph), 3.58 (s, 3H, Ph–O–CH_3). ^{13}C NMR [CD_3Cl, ppm]: δ 120.32–141.95 (Ar–C), 29.62 (Ph–O–CH_3), 38.4 (CH_2–Ph). ^{119}Sn NMR [CD_3Cl, ppm]: −145.32.

2.3.7. $[Me_3Sn(C_9H_{11}SeO_2)]_n$ (7). The procedure is similar to that of **1**, 4-isopropylbenzeneseleninic acid (0.231 g, 1 mmol), sodium ethoxide (0.068 g, 1 mmol), and trimethyltin chloride (0.199 g, 1 mmol) were reacted for 12 h at 50°C. Recrystallized from ether, transparent colorless crystals were formed. Yield: 62%; m.p. 156–159°C. Anal. Calcd for $C_{12}H_{20}SnO_2Se$: C, 36.58; H, 5.12. Found (%): C, 36.31; H, 5.21. IR (KBr, cm^{-1}): ν(Sn–C), 546.43; ν(Sn–O), 428.40. ^{1}H NMR [CD3Cl, ppm]: δ 7.26–7.61 (m, 4H, –Ph), 1.23 (s, 6H, CH_3), 2.91–2.98 (m, 1H, –CH), 0.58 (s, 9H, Sn–CH_3). ^{13}C NMR [CD_3Cl, ppm]: δ 129.62, 129.68, 138.63, 138.65 (Ar–C), 28.32 (–CH–), 18.25 (CH_3), 17.7 (Sn–CH_3). ^{119}Sn NMR [CD_3Cl, ppm]: −147.24.

2.3.8. $[Ph_3Sn(C_9H_{11}SeO_2)]_n$ (8). The procedure is similar to that of **1**, 4-isopropylbenzeneseleninic acid (0.231 g, 1 mmol), sodium ethoxide (0.068 g, 1 mmol), and triphenyltin chloride (0.385 g, 1 mmol) were reacted for 12 h at 50°C. Recrystallized from ether, white powder was formed. Yield: 62%; m.p. 235–238°C. Anal. Calcd for $C_{27}H_{26}SnO_2Se$: C, 55.90; H, 4.52. Found (%): C, 56.22; H, 4.28. IR (KBr, cm^{-1}): ν(Sn–C), 543.71 ν(Sn–O), 448.06. ^{1}H NMR [CD_3Cl, ppm]: δ 7.21–7.75 (m, 19H, –Ph), 1.25 (s, 6H, CH_3), 2.91–2.97 (m, 1H, –CH). ^{13}C NMR [CD_3Cl, ppm]: δ 129.21–139.93 (Ar–C), 25.68 (CH), 17.91(CH_3). ^{119}Sn NMR [CD_3Cl, ppm]: −135.73.

2.3.9. $[(PhCH_2)_3Sn(C_9H_{11}SeO_2)]_n$ (9). The procedure is similar to that of **1**, 4-isopropylbenzeneseleninic acid (0.231 g, 1 mmol), sodium ethoxide (0.068 g, 1 mmol), and $(PhCH_2)_3SnCl$ (0.427 g, 1 mmol) were reacted for 12 h at 50°C. Recrystallized from ether, white powder was formed. Yield: 62%; m.p. 221–224°C. Anal. Calcd for $C_{30}H_{32}SnO_2Se$: C, 57.91; H, 5.18. Found (%): C, 57.65; H, 5.24. IR (KBr, cm^{-1}): ν(Sn–C), 547.86 ν(Sn–O), 438.57. ^{1}H NMR [CD_3Cl, ppm]: δ 7.19–7.75 (m, 19H, –Ph), 1.26 (s, 6H, CH_3), 2.89–2.95 (m, 1H, –CH–). ^{13}C NMR [CD_3Cl, ppm]: δ130.63–142.12 (Ar–C), 27.24 (–CH–), 17.52 (CH_3), 38.2 (CH_2–Ph). ^{119}Sn NMR [CD_3Cl, ppm]: −122.93.

3. Results and discussion

3.1. *Syntheses*

The syntheses of **1**–**9** are shown in scheme 1.

3.2. *IR spectra*

The vibrational frequencies of interest are those associated with Sn–O, Se–O, and Sn–C. Bands at 2700–3000 cm^{-1}, which appear in the free ligands as ν(O–H) stretching vibrations, are not observed in **1**–**9**, indicating metal–ligand bond formation through these sites. Strong absorptions at 428–475 cm^{-1}, which are absent in the spectra of free ligand, are assigned to Sn–O stretch. Strong bands at 712–774 cm^{-1} in the spectra are assigned to Se–O stretch. Weak bands at 535–580 cm^{-1} for **1**–**9** are assigned to ν(Sn–C), indicating a non-linear *trans*-configuration of C–Sn–C. All these values are consistent with those detected in organotin derivatives [15–17].

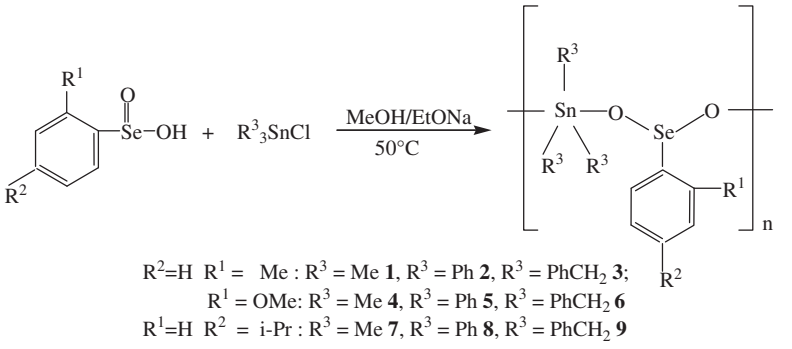

R^2=H R^1 = Me : R^3 = Me **1**, R^3 = Ph **2**, R^3 = $PhCH_2$ **3**;
R^1 = OMe: R^3 = Me **4**, R^3 = Ph **5**, R^3 = $PhCH_2$ **6**
R^1=H R^2 = i-Pr : R^3 = Me **7**, R^3 = Ph **8**, R^3 = $PhCH_2$ **9**

Scheme 1. Syntheses of **1**–**9**.

3.3. *NMR spectra*

^{1}H NMR spectra show the expected integrations and peak multiplicities. In the free ligand, the resonances at 8.5–10 ppm, which are absent in the spectra of the complexes, indicate the removal of $^-SeO_2H$ protons and the formation of Sn–O bonds, in agreement with the IR data. The ^{13}C NMR spectra of all complexes show a significant downfield shift of all carbon resonances compared to the free ligands because of electron-density transfer from the ligands to tin [18, 19]. The ^{119}Sn NMR data of all the complexes show only one resonance between −122.93 and −152.78 ppm. As reported in the literature [20], δ values for ^{119}Sn NMR spectra in the −90 to −190 ppm range have been associated with five-coordinate tin, confirmed by X-ray crystallography.

3.4. *Description of crystal structures of 1, 2, 4, 5, 7, and 8*

Selected bond lengths and angles for **1**, **2**, **4**, **5**, **7**, and **8** are given in tables 3–5, respectively, and repeating units of complexes are illustrated in figures 1–6, respectively. In the crystalline state, these complexes adopt infinite 1-D polymeric chain structures with a five-coordinate tin, generated by $RSeO_2^-$ and Sn center. These structures are very similar to $[R_3SnO_2P(OC_2H_5)_2]_n$ [21]. The Sn exists in a slightly distorted trigonal bipyramidal environment with the basal plane defined by three carbon groups and two O atoms derived from two symmetry related, bridging $RSeO_2^-$ ligands, the sum of the trigonal angles is 360°, the corresponding axial-Sn-axial angles [O(1)–Sn(1)–O(2)$^{\#1}$ 173.70(9)°, for **1**; O(2)$^{\#1}$–Sn(2)–O(4) 174.2(2)°, for **2**; O(1)–Sn(1)–O(2) 172.59(8)°, for **4**; O(7)–Sn(1)–O(6) 177.2(2)°, for **5**; O(2)–Sn(1)–O(3) 171.4(11)°, for **7**; O(2)–Sn(1)–O(1)$^{\#1}$ 174.45(9)°, for **8**], and the Sn lie in the plane of the three carbons within experimental error [22]. The $RSeO_2^-$ symmetrically bridges two Sn's forming indistinguishable Sn–O bond lengths [Sn(1)–O(1) 2.246(3) Å, Sn(1)–O(2)$^{\#1}$ 2.262(3) Å, for **1**; Sn(1)–O(1) 2.192(4) Å, Sn(1)–O(3) 2.193(5) Å, Sn(2)–O(2)$^{\#1}$ 2.220(5) Å, Sn(2)–O(4) 2.225(5) Å, for **2**; Sn(1)–O(1) 2.226(2) Å, Sn(1)–O(2) 2.265(2) Å; for **4**; Sn(1)–O(7) 2.214(6) Å, Sn(1)–O(6) 2.229(6) Å, Sn(2)–O(9) 2.187(6) Å, Sn(2)–O(10) 2.218(6) Å, for **5**; Sn(1)–O(2) 2.25(2) Å, Sn(1)–O(3) 2.31(3) Å, for **7**; Sn(1)–O(2) 2.218(2) Å, Sn(1)–O(1)$^{\#1}$ 2.227(2) Å, for **8**], producing six 1-D infinite chain structures as shown in figures 1–6, respectively. The symmetrical bridging mode of coordination of $RSeO_2^-$

Table 3. Selected bond lengths (Å) and angles (°) for **1** and **2**.

Complex **1**			
Sn(1)–C(10)	2.118(4)	Sn(1)–C(11)	2.121(4)
Sn(1)–C(9)	2.117(4)	Sn(1)–O(1)	2.246(3)
Sn(1)–O(2)$^{\#1}$	2.262(3)	Se–O(1)	1.680(3)
Se–O(2)	1.692(3)	Se–C(6)	1.946(4)
O(1)–Sn(1)–O(2)$^{\#1}$	173.70(9)	O(1)–Se–O(2)	173.70(9)
C(10)–Sn(1)–C(9)	120.91(17)	O(2)–Se–C(6)	99.88(14)
C(10)–Sn(1)–C(11)	118.07(17)	C(9)–Sn(1)–C(11)	120.97(15)
Complex **2**			
Sn(1)–C(27)	2.119(7)	Sn(1)–O(1)	2.192(4)
Sn(1)–C(21)	2.127(8)	Sn(1)–O(3)	2.193(5)
Sn(1)–C(15)	2.245(6)	Se(1)–O(1)	1.688(5)
Sn(2)–O(2)$^{\#1}$	2.220(5)	Sn(2)–O(4)	2.225(5)
O(1)–Sn(1)–O(3)	174.81(19)	Se(1)–O(2)	1.693(5)
C(27)–Sn(1)–C(21)	124.4(3)	O(1)–Se(1)–C(1)	98.3(3)
C(27)–Sn(1)–C(15)	118.2(3)	O(1)–Se(1)–O(2)	102.4(3)

Symmetry code for **1**: $^{\#1}-x+1/2,\ y+1/2,\ -z+1/2$.
Symmetry code for **2**: $^{\#1}-x+1/2,\ -y+2,\ z-1/2$.

Table 4. Selected bond lengths (Å) and angles (°) for **4** and **5**.

Complex **4**			
Sn(1)–C(3)	2.113(4)	Sn(1)–O(1)	2.226(2)
Sn(1)–C(1)	2.119(4)	Sn(1)–O(2)	2.265(2)
Sn(1)–C(2)	2.121(4)	Se(1)–O(2)	1.677(2)
O(1)–Sn(1)–O(2)	172.59(8)	Se(1)–O(1)$^{\#1}$	1.692(2)
C(3)–Sn(1)–C(1)	119.82(18)	O(2)–Se(1)–O(1)$^{\#1}$	105.07(11)
C(3)–Sn(1)–C(2)	121.57(17)	C(1)–Sn(1)–C(2)	118.59(17)
Complex **5**			
Sn(1)–C(33)	2.118(9)	Sn(1)–O(7)	2.214(6)
Sn(1)–C(45)	2.141(10)	Sn(1)–O(6)	2.229(6)
Sn(1)–C(39)	2.154(9)	Se(1)–O(3)	1.673(7)
Sn(2)–O(9)	2.187(6)	Sn(2)–O(10)	2.218(6)
O(7)–Sn(1)–O(6)	177.2(2)	Se(1)–O(1)	1.692(2)
C(33)–Sn(1)–C(45)	122.5(4)	O(4)–Se(2)–O(6)	100.6(3)
C(33)–Sn(1)–C(39)	119.5(4)	O(3)–Se(1)–C(1)	97.3(4)

Symmetry code for **4**: $^{\#1}-x+1,\ y+1/2,\ -z+1/2$.

is reflected in the experimentally equivalent Se–O bonds distances [Se–O(1) 1.680(3) Å, Se–O(2) 1.692(3) Å, for **1**; Se(1)–O(1) 1.688(5) Å, Se(1)–O(2) 1.693(5) Å, for **2**; Se(1)–O(2) 1.677(2) Å, Se(1)–O(1)$^{\#1}$ 1.692(2) Å, for **4**; Se(1)–O(3) 1.673(7) Å, Se(1)–O(1) 1.707(7) Å, for **5**; Se(2)–O(3) 1.68(3) Å, Se(2)–O(4) 1.69(3) Å, for **7**; Se(1)–O(1) 1.679(2) Å, Se(1)–O(2) 1.689(2) Å, for **8**]. The Se geometry is pyramidal owing to the presence of a stereochemically active lone pair of electrons; there is no evidence of interaction between Sn and Se [5]. Although **1**, **2**, **4**, **5**, **7,** and **8** are all infinite 1-D polymeric chain structures, these complexes have different coordination modes. Sn of **1**, **4**, **7**, and **8** linked by ligands in *syn–anti* conformation are arranged in zig-zag chains; Sn of **2** and **5** linked by ligands in *anti–anti* conformation are arranged in collinear chains [23].

Table 5. Selected bond lengths (Å) and angles (°) for **7** and **8**.

Complex **7**			
Sn(1)–C(34)	2.00(4)	Sn(1)–O(2)	2.25(2)
Sn(1)–C(36)	2.09(5)	Sn(1)–O(3)	2.31(3)
Sn(1)–C(35)	2.19(3)	Se(2)–O(3)	1.68(3)
Se(2)–O(4)	1.69(3)	O(2)–Sn(1)–O(3)	171.4(11)
C(34)–Sn(1)–C(36)	122.7(18)	C(34)–Sn(1)–C(35)	116.8(19)
C(36)–Sn(1)–C(35)	120.4(17)	O(3)–Se(2)–O(4)	105.1(14)
Complex **8**			
Sn(1)–C(13)	2.124(4)	Sn(1)–O(2)	2.218(2)
Sn(1)–C(1)	2.131(4)	Sn(1)–O(1)$^{\#1}$	2.227(2)
Sn(1)–C(7)	2.130(4)	Se(1)–O(1)	1.679(2)
O(1)–Sn(1)$^{\#2}$	2.227(2)	Se(1)–O(2)	1.689(2)
O(1)–Se(1)–O(2)	103.56(13)	O(1)–Se(1)–C(19)	99.01(14)
Se(1)–O(2)–Sn(1)	136.83(13)	O(2)–Sn(1)–O(1)$^{\#1}$	174.45(9)

Symmetry code for **8**: $^{\#1}-x+1/2,\ y-1/2,\ -z+1/2$; $^{\#2}-x+1/2,\ y+1/2,\ -z+1/2$.

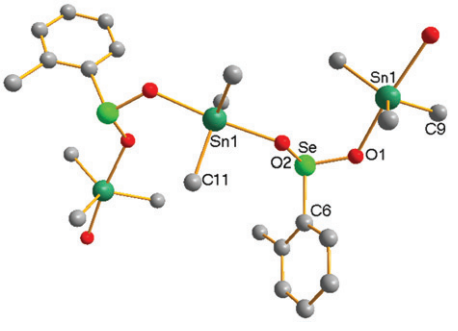

Figure 1. The molecular structure of **1**.

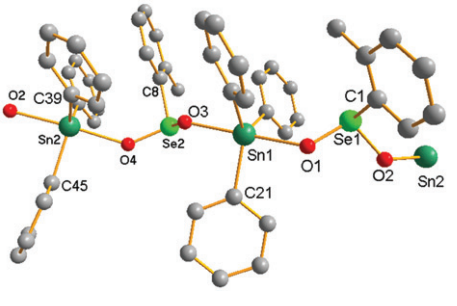

Figure 2. The molecular structure of **2**.

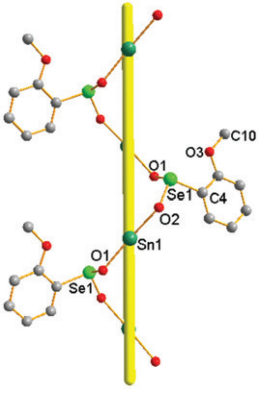

Figure 3. The molecular structure of **4**.

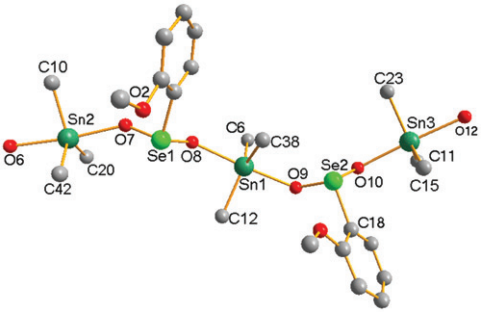

Figure 4. The molecular structure of **5** (for clarity, the excessive carbons of benzene rings are omitted).

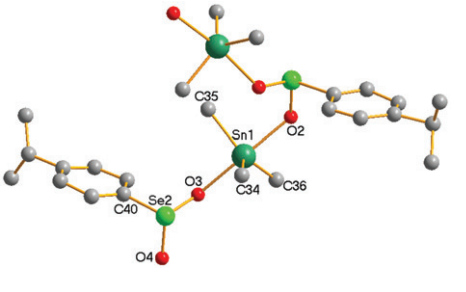

Figure 5. The molecular structure of **7**.

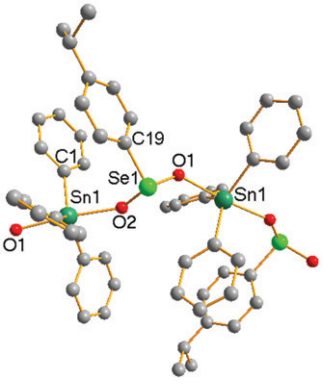

Figure 6. The molecular structure of **8**.

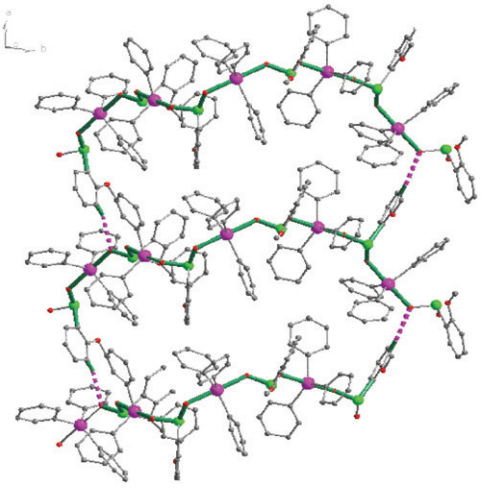

Figure 7. 2-D metal framework of **5** made up of intermolecular C–H···O interactions.

Furthermore (figure 7), the supramolecular structure of **5** is a 2-D network linked by intermolecular C–H···O weak interactions. The C–H···O distances are 2.619 Å, smaller than the sum of van der Waals radii (2.72 Å) [24].

3.5. *TGA of crystal structures of 1–9*

To study the stabilities of **1**–**9**, TGA was performed from 50°C to 500°C under N_2 atmosphere. The TGA curves of **1**–**9** exhibit one continuous weight loss from 190–390°C. In general, **1**–**9** exhibit good thermal stability [25].

Table 6. Concentrations of **1** and **2** to obtain 50% inhibition of SMMC-7721, P388, and MCF-7 proliferate activities.

	IC_{50} ($ng\,mL^{-1}$)		
Complex	SMMC-7721	P388	MCF-7
1	9 ± 0.13	34 ± 0.18	45
2	22 ± 0.45	17 ± 0.56	62
CPT	13700	185	699

3.6. *Antitumor activities* in vitro *of organotin complexes*

The cytotoxicities of **1** and **2** were performed using five cancer lines (SMMC-7721, P388, and MCF-7) and the results, in terms of IC_{50}, were compared with the reference standard cisplatin (CPT). The corresponding IC_{50} values for SMMC-7721, P388, and MCF-7 cell lines are listed in table 6. From the IC_{50} values (table 6), **1** and **2** show very significant potency *in vitro* against the SMMC-7721, P388, and MCF-7 cell lines and their antitumor activities are much higher than that of the clinically used cisplatin (CPT) [26, 27]. The relative effectiveness of the antitumor activities shows that the different complexes act against the same cell with different effects, while the same complex acts against the different cells also with different effects. The results indicate that complexes act against cells selectively.

4. Conclusion

A series of triorganotin(IV) complexes based on 2-methylbenzeneseleninic acid, 2-methoxybenzeneseleninic acid, and 4-isopropylbenzeneseleninic acid have been synthesized. Both spectra and crystal structures show that when sub-areneseleninic acids react with triorganotin(IV) chloride, they can form 1-D infinite chain structures through substituting of chloride. These structures are very similar to corresponding triorganotin phosphonates. The geometry of tin in each complex is five-coordinate in a trigonal bipyramid geometry. The TGA of **1**–**9** show stability until 190°C. Antitumor activities of **1** and **2** have been tested, showing higher cytotoxic activity against the cancer cell lines SMM-7221, MCF-7, and P388.

Supplementary material

CCDC Nos 837256 **1**, 837260 **2**, 837258 **4**, 837257 **5**, 838320 **7**, and 838319 **8** contain the supplementary crystallographic data for this article. These data can be obtained free of charge *via* http://www.ccdc.cam.ac.uk/conts/retrieving.html, or from the Cambridge Crystallographic Data Centre, 12 Union Road, Cambridge, CB2 1EZ, UK; Fax: (+44) 1223-336-033; E-mail: deposit@ccdc.cam.ac.uk.

Acknowledgments

We thank the Natural Science Foundation of China (20971096) and Natural Science Foundation of Shandong Province (ZR2010BL019) for the financial support.

References

[1] V. Chandrasekhar, S. Nagendran, V. Baskar. *Coord. Chem. Rev*., **235**, 1 (2002).
[2] C.N.R. Rao, S. Natarajan, R. Vaidhyanathan. *Angew. Chem*., **116**, 1490 (2004).
[3] S.K. Duboy, U. Roy. *Appl. Organomet. Chem*., **17**, 3 (2003).
[4] C.L. Ma, J.F. Sun. *Dalton Trans*., **12**, 1785 (2004).
[5] C.L. Ma, Y.F. Han, R.F. Zhang, D.Q. Wang. *Dalton Trans*., **12**, 1832 (2004).
[6] R. García-Zarracino, H. Höpfl. *J. Am. Chem. Soc*., **127**, 3120 (2005).
[7] D. Dakternieks, A. Duthie, B. Zobel, K. Jurkschat, M. Schürmann, E.R.T. Tiekink. *Organometallics*, **21**, 647 (2002).
[8] V. Chandrasekhar, M.G. Muralidhara, K.R.J. Thomas, E.R.T. Tiekink. *Inorg. Chem*., **31**, 4707 (1992).
[9] A.J. Mukherjee, S.S. Zade, H.B. Singh, R.B. Sunoj. *Chem. Rev*., **110**, 4351 (2010).
[10] G. Mugesh, W.W.D. Mont, H. Sies. *Chem. Rev*., **101**, 2125 (2001).
[11] K.P. Bhabak, G. Mugesh. *Acc. Chem. Res*., **43**, 1408 (2010).
[12] H.J. Thompson, A. Wilson, J. Lu, M. Singh, C. Jiang, P. Upadhyaya, K. El-Bayoumy, C. Ip. *Carcinogenesis*, **15**, 183 (1994).
[13] K. Kloc, J. Mlochowski, L. Syper. *Liebigs Ann. Chem*., **54**, 811 (1989).
[14] H.J. Reich, C.P. Jasperse. *J. Org. Chem*., **53**, 2389 (1988).
[15] W. Diallo, C.A.K. Diop, L. Diop, M.F. Mahon, K.C. Molloy, U. Russo, M. Biesemans, R. Willem. *J. Organomet. Chem*., **692**, 2187 (2007).
[16] D. Kovala-Demertzi, V.N. Dokorou, J.P. Jasinski, A. Opolski, J. Wiecek, M. Zervou, M.A. Demertzis. *J. Organomet. Chem*., **690**, 1800 (2005).
[17] C.L. Ma, M.Q. Yang, R.F. Zhang. *Inorg. Chim. Acta*, **361**, 2979 (2008).
[18] H.J. Reich, C.P. Jasperse. *J. Org. Chem*., **53**, 2389 (1988).
[19] The pKa values for 1 and 2 are 4.88 and 5.05, respectively, in aqueous solution; J.D. McCullough, E.S. Gould. *J. Am. Chem. Soc*., **71**, 674 (1949).
[20] J. Holecek, M. Nadvornik, K. Handlir, A. Lycka. *J. Organoment. Chem*., **315**, 299 (1986).
[21] R.F. Zhang, M.Q. Yang, C.L. Ma. *J. Organoment. Chem*., **693**, 2551 (2008).
[22] C.L. Ma, B.Y. Zhang, S.L. Zhang, R.F. Zhang. *J. Organomet. Chem*., **696**, 2165 (2011).
[23] S. Konar, P.S. Mukherjee, M.G.B. Drew, J. Ribas, N.R. Chaudhuri. *Inorg. Chem*., **42**, 2545 (2003).
[24] A. Bondi. *J. Phys. Chem*., **68**, 441 (1964).
[25] C.L. Ma, G.R. Tian, R.F. Zhang. *Inorg. Chem. Commun*., **9**, 882 (2006).
[26] L.B. Chen, H. Lu, J. Zang, C. Wang. *J. Medi. Postgradu*., **17**, 685 (2004).
[27] T.A.K. Al-Allaf, L.J. Rashan. *Eur. J. Med. Chem*., **33**, 817 (1998).